Studies of the Cerenkov emission angle reconstruction. Part 2

P. Schiavon

COMPASS / RICH / PS / Report 3.a

27 / 10 / 97 - rev. 27/11/97 (in progress)

1 Note :

For the definitions of the reference systems and the geometry of the apparatus refer to the Reports COMPASS / RICH / PS / Report 1 and 2.

2 Photon optics :

a) The Cerenkov photons are emitted (at least as a first approximation) with an uniform distribution in distance (s) along the particle path length inside the radiator and in angle (ϕ) around the particle trajectory;
for a particle trajectory normal to the mirror surface, the photons fill a circular area on the mirror with a density decreasing (as a first approximation) as $1/r$, where r is the distance on the mirror surface from the particle impact point;
after reflection, the photons 'focalize' on the detector surface around a closed line, the *ring*.

b) To better understand this focalization, we can follow two lines :

b-1) We select photons emitted at a fixed ϕ around the particle trajectory and at different s;
their trajectories are all parallel and belong to the same plane; in geometrical optics terms, they come all from a point source at infinity and should (in the small angle approximation) converge in one focal point, on the mirror axis, at a distance of $R/2$ from the mirror surface (R is the mirror radius); in this case, the mirror axis is defined as the line through the mirror centre and parallel to the photon trajectories (see fig.1).
Taking into account large angles and spherical aberrations, the reflected photons stay no longer in the same plane, but lay on a slightly curved surface on which the trajectories cross each other at differents points; we can define a 'centroid' as the point to which the sum squared of the distances from the trajectories is a minimum ('focus').
As the ϕ angle is varied around the particle trajectory, the 'focus' changes its position in space, following a typical closed line (*space ring*) (see fig.2);

b-2) We select photons emitted at a fixed s and at different ϕ around the particle trajectory,

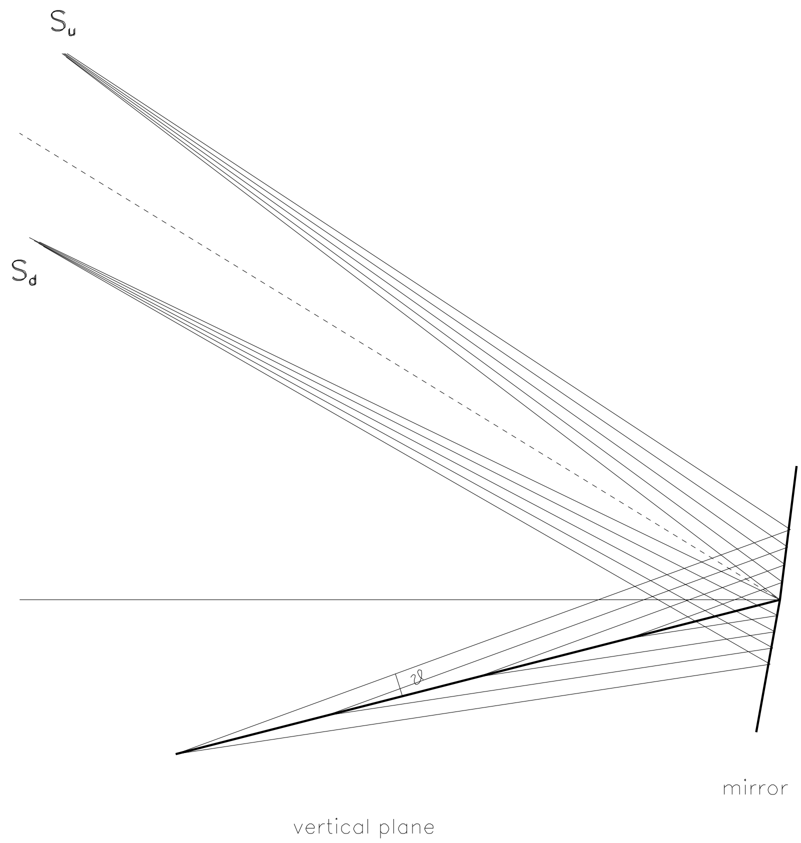

Figure 1: Geometry for the case of photons emitted at fixed ϕ; in this example the particle (thick line) and the photons lie in the vertical (yz) plane: photons emitted at different distances along the particle path, 'focuse' in the points S_u or S_s of the *space ring*.

the emission point acts as a point source at a distance from the mirror surface smaller than the focal length of the mirror, $R/2$; in the small angle approximation, after reflection, the photons all emerge from a point, the *virtual image*, beyond the mirror surface (see fig.3).

For large angles, taking into account spherical aberrations, there is no more a *virtual image* point, but a region where the virtual reflected photon trajectories come more or less closer each other at different depths; the conical surface of the incoming photon trajectories is reflected into a conical surface with a cross section which is a distorted ellipse. As the emission position s is varied along the particle path, the reflected conical surface varies in shape and *virtual image* position; they cross each other approximatively along a closed space line, the *space ring* defined above (see fig.2).

b-3) Assume that we position the detector surface to fit the *space ring* (in fact an average of many different *space rings* due to the various particle configurations); the shadow of the *space ring* onto the detector surface (i.e. the impact points on the detector surface of the reflected photons) is what we call the *ring*. It is clear that the larger the distance between a *space ring* point and the detector surface, the larger the dispersion of the photon impact points around the corresponding point of the *ring* (see fig.2 (b) and fig.4).

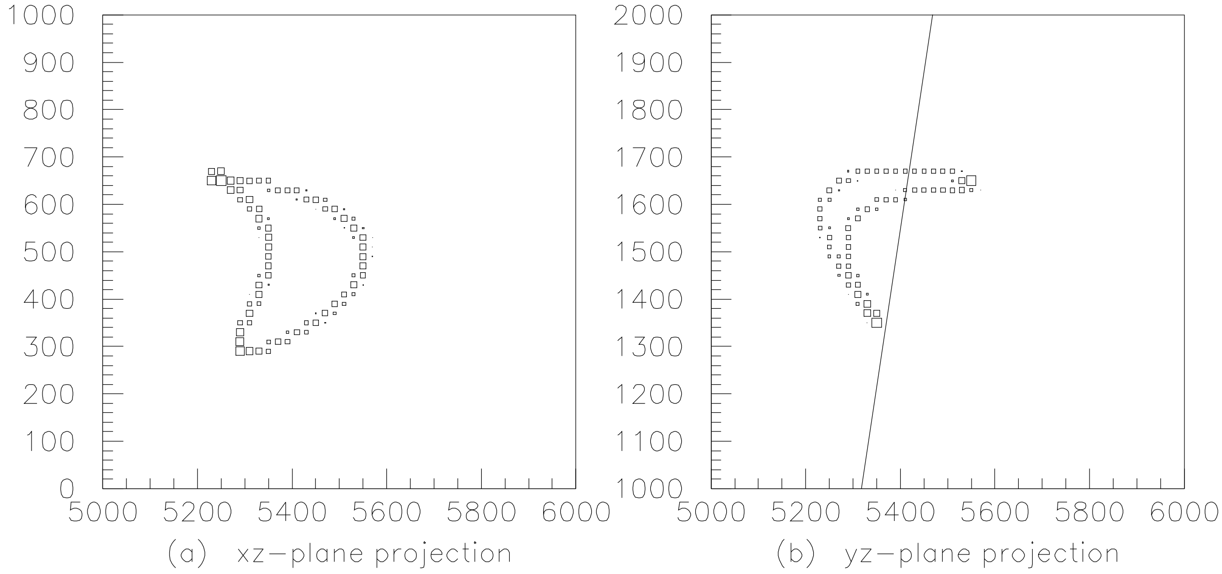

Figure 2: *Space ring* projections on the horizontal (a) and on the vertical (b) planes for photons emitted by a particle of $\beta = 1$ and angles $\theta = 8.$ and $\phi = 0.$ degrees. In (b) the line represent a possible position of the detector plane. Note that a very large (3000) number of photons has been used for a detailed description of the *ring*.

3 Reconstruction procedure :

a) Let's take the following definitions :

- the particle *impact parameter*: the (orthogonal) distance between the particle trajectory (as inside the radiator) and the centre of the mirror spherical surface.
- the *reflected particle* trajectory: the particle trajectory, as if reflected by the mirror surface like a light ray;
- the *particle plane*: the plane defined by the true perticle and *reflected particle* trajectories; it contains the mirror centre.
- the particle *orthogonal plane*: the plane orthogonal to the *reflected particle* trajectory through the point where this trajectory hits the detector plane.

b) To understand the relationship between emission angle and *ring* shape assume the photons emitted as in b-2) of section 2 above (fixed s) and look at what the *ring* is on the particle *orthogonal plane*.

b-1) If s is such that the photons are emitted from the point where the particle hits the mirror ($s = s_{max}$), there are no spherical aberrations and the shape of the *ring* is exactly a circle; if $s < s_{max}$, down to $s = 0.$ (radiator entrance), the *ring* shape is, with good approximation, an ellipse, at least in the sense discussed in b-3), with the ratio of the minor to the major axis increasing towards 1 as s approaches 0. Moreover, if on the particle *orthogonal plane* we define a reference system (*pa*-reference) in which the y-axis is along the intersection between the *orthogonal plane* and the *particle plane* and the z-axis along the *reflected particle* path, the 'ellipse' is oriented with its major axis along x and the minor axis along y and symmetric with respect to the y-axis.

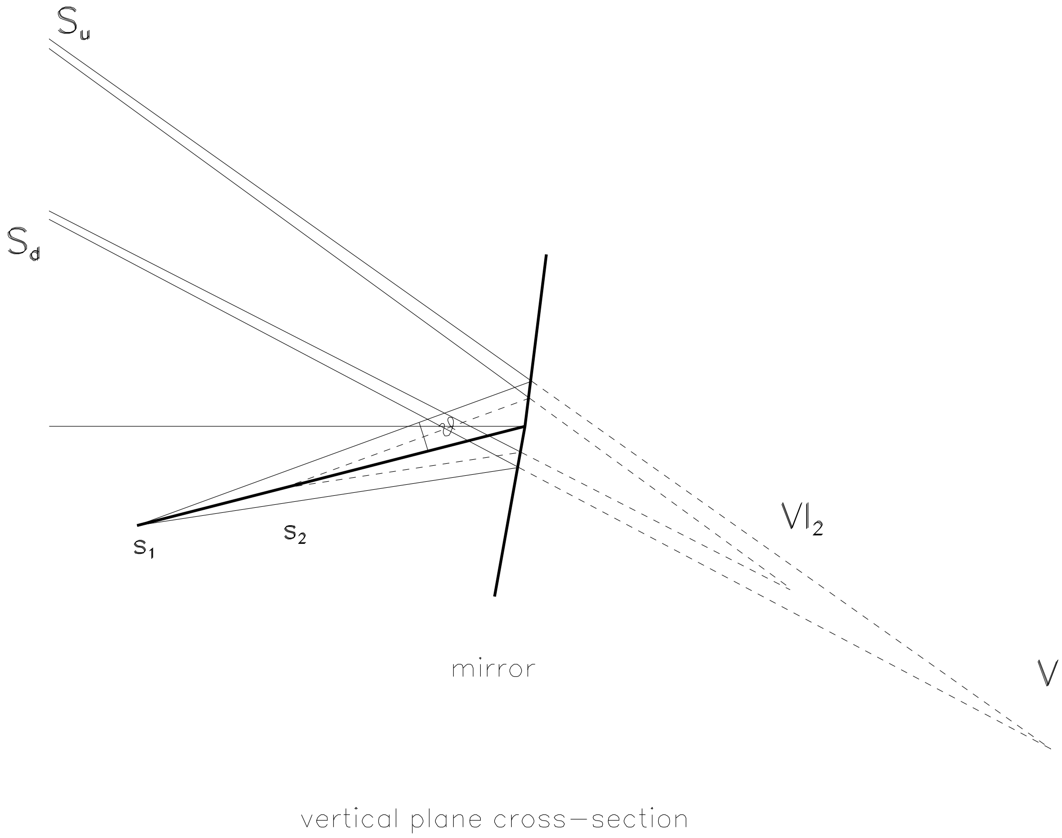

Figure 3: Geometry for the case of photons emitted at fixed s; two different emission positions are considered (s_1 and s_2) to which correspond the two 'virtual images' VI_1 and VI_2; vertival (yz) plane cross-section.

b-2) On the detector surface, which is in general rotated with respect to the *orthogonal plane*, for all s, the *ring* has then an approximate elliptical form, in the sense that the different elliptical shapes for different s, as outlined above, combine together.
Fitting an ellipse to the data points, one makes an average over hits of photons emitted at different s and we assume that this is equivalent to fitting the ellipse to the hits of photons emitted at the average s, i.e. $s_{max}/2$. Then we relate the fitted ellipse parameters to the Cerenkov emission angle. It is clear that the shape and the orientation of the 'ellipse' depend on the emission angle value as well as on the particle trajectory parameters.

c) From the point of view of the technical details the procedure is the following :

c-1) On the detector surface the elliptical shape is rather approximate and not too far from that of a circle (see fig. 4 (a)); this means that a fit of the form with 5 parameters to be determined (semi-major and -minor axes, x- and y-coordinates of the centre and orientation) is rather unstable;
a better solution is that of fitting the 'ellipse' as it appears when 'projected' on the *orthogonal plane* (in the *pa*-reference) where only 3 parameters are needed : semi-major(a) and -minor(b) axes and y-coordinate of the centre (y_c).
To work out how to 'project' the 'ellipse' onto the *orthogonal plane*, we assume that all the photons are emitted from the middle point of the particle path inside the radiator (s

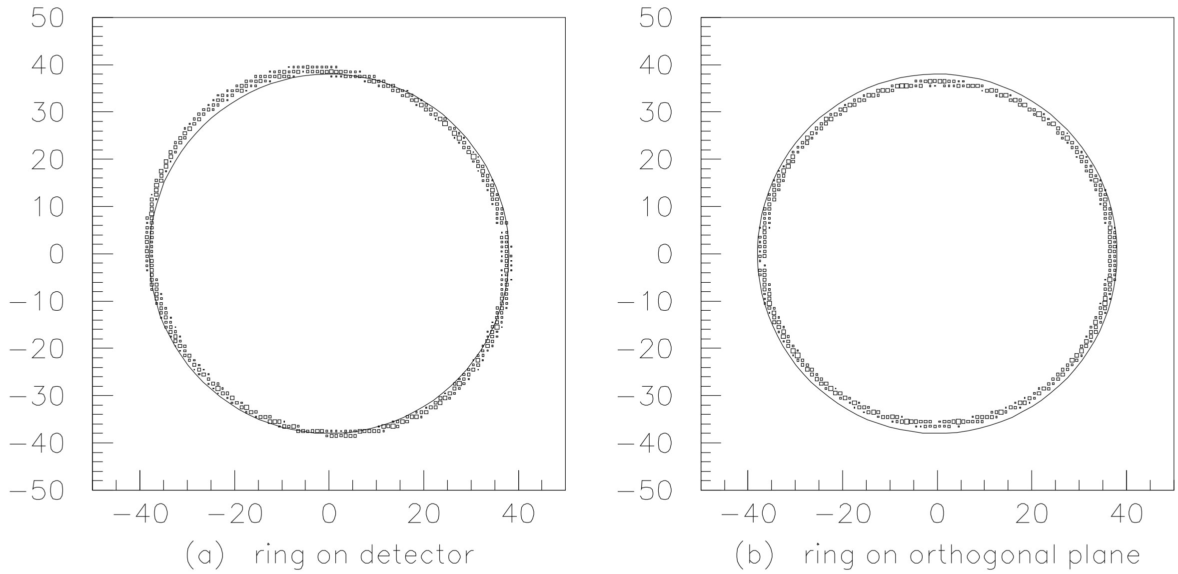

Figure 4: (a) *ring* on the detector plane, (b) *ring* on the *orthogonal plane* for the same particle as in fig.2; the centre of the plot is in the *reflected particle* 'hit' on the detector surface. The circle is to guide the eye only. Note that the radial distance has been reduced to the 20% of the real length to enhance the spread of the photon impact points.

$= s_{max}/2.$) and then we correlate the intersections of the approximate conical surface (as described in b-2)) with both the detector surface and the *orthogonal plane* surface; the result is poorly dependent on d_{vd}, the distance between the approximate *virtual image* point of $s_{max}/2.$ and the *reflected particle* impact point on the detector along its path; in conclusion the data points are on the detector surface, but the ellipse is parametrized as a function of the three parameters above and the three angles (known for each particle) defining the relative orientation of the *orthogonal plane* and the detector surface.

c-2) Let's use in the following d_{em}, the distance between the photon emission point and the particle impact point on the mirror along its path, instead of s ($d_{em} = 0.$ for $s = s_{max}$) (see fig.5);
In the case of $d_{em} = 0.$ as described in d-1) above, the radius of the fitted circle divided by the distance between the particle impact point on the mirror and the *reflected particle* impact point on the detector surface (d_{md}) gives exactly the tangent of the emission angle.
In the general case, the lines labelled (1), (2) and (3) in fig. 6 represent the reflected paths of photons emitted at d_{em} = max (1), d_{em} = max/2 (2) and $d_{em} = 0.$ (3); on the *particle plane* the fitted ellipse minor axis (b_f) corresponds to half the distance B_u - B_d; to compute θ_C we need to know half the distance C_u - C_d (= b_{corr}), applying the corrections Δb_u and Δb_d; at a first order approximation

$$\tan\theta_C \simeq \theta_C = \frac{b_{corr}}{d_{md}} \qquad\qquad b_{corr} = b_f - \frac{\Delta b_u + \Delta b_d}{2}$$

$$b_{corr} = b_f - \theta_C d_{em}(1. - \frac{2.\, d_{md}}{R\cos\alpha});$$

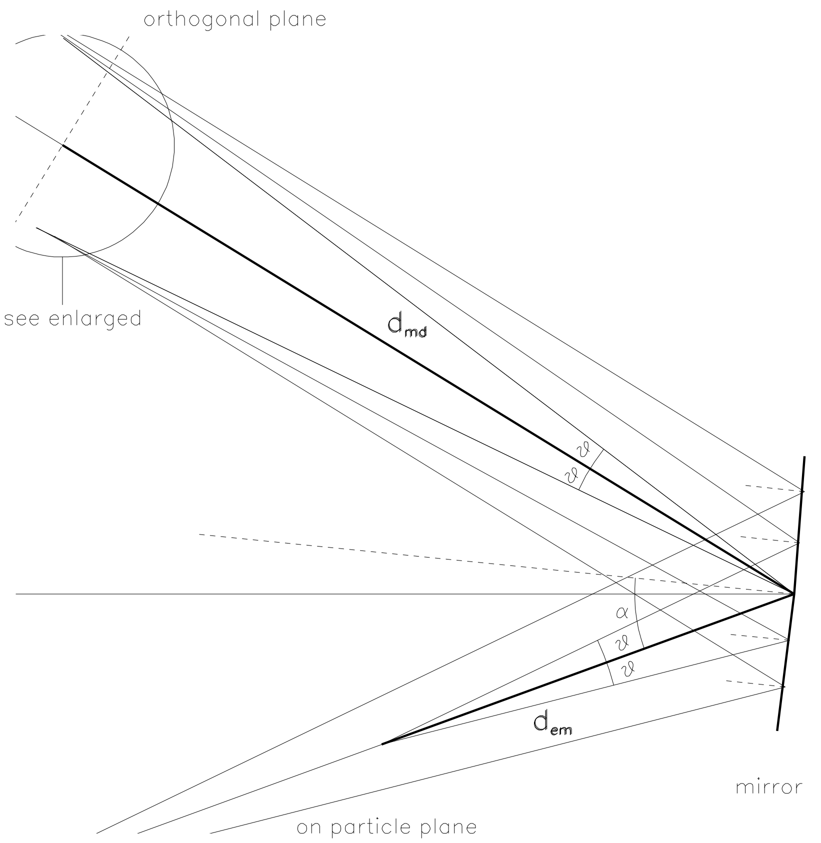

Figure 5: Geometry of photons emitted at $d_{em} = 0.$ and $d_{em} = \max/2$; angles and distances used in the θ_C reconstruction are shown. Fig. 6 blows up the region in the circle.

α is the angle, on the *particle plane*, between the particle trajectory and the normal to the mirror at the particle impact point; combining the three relations we get :

$$\theta_C = \frac{b_f}{d_{md}} \frac{1.}{[1. + d_{em}(1./d_{md} - 2./R\cos\alpha)]} \tag{1}$$

where b_f is the result of the fit and d_{md} and α are calculated for each particle; because d_{em} is not known, we assume as usual the middle point ($d_{em} = s_{max}/2. = d_{1/2}$);

4 Results :

The results are summarized in Table 1.

a) In the simulation we have used a sample of particles from a file of LEPTO generated events as described in COMPASS / RICH / PS / Report 1, with a θ_C distribution peaked at rather high values (column 2 of table 1); moreover, for comparison, data are also available from a sample of particles with θ_C uniformely distributed between 10. and 60. $mrad$ ($\beta = 1.$ corresponds to $\theta_C = 55.8$ $mrad$ in the case of RICH 1) (column 4 in table 1).
To evaluate the *ring* resolution in θ_C, a fixed number of 30 photons per particle has been

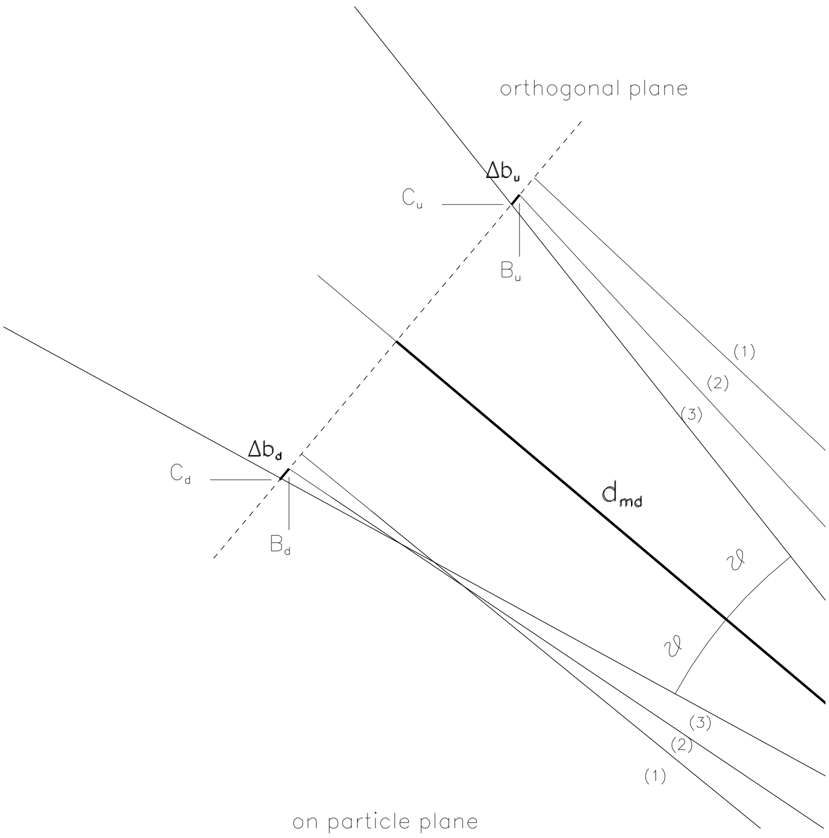

Figure 6: The relevant geometry in the region of the *orthogonal plane*. On the *particle plane*, the lines labelled (1), (2) and (3) represent the reflected paths of photons emitted at d_{em} = max (1), d_{em} = max/2 (2) and $d_{em} = 0.$ (3); Δb_u and Δb_d are the correction to apply to the fitted ellipse minor axis to compute θ_C. See the text for more details.

simulated.

Spherical aberrations in the reconstruction are due to the fact that, in equation (1), d_{em} is fixed to $d_{1/2}$; to evaluate the resulting resolution in the θ_C angle, we differentiate equation (1) with respect to d_{em}; then :

$$\frac{\sigma_\theta}{\theta_C} = \frac{-(1./d_{md} - 2./R\cos\alpha)}{[1. + d_{1/2}(1./d_{md} - 2./R\cos\alpha)]} \tag{2}$$

which doesn't depend on θ_C and little on particle geometry.
The use of expression (2) gives a result independent of the emission angle distribution (column 3 in table 1).
In the fourth row of the table 1 is shown for comparison the resolution obtainable using the reconstruction method described in COMPASS / RICH / PS / Report 2; the figure is fairly better than that of row 1.
Note that in this exercise no experimental resolution (pixel) has been taken into account; the last row of table 1 shows the contribution of the experimental resolution on the measured position of the photon hits on the detector assuming a pixel of 8. $mm \times 8.\ mm$ as expected.

	physical distr.		uniform distr.
	σ_θ μrad	σ_θ/θ	σ_θ μrad
fit on orth. pl. with corr.	144.	.0031	120.
fit on orth. pl. NO corr.	∼510.		∼400.
fit on det. pl. with corr.	280.	.0057	147.
direct angle reconstr.	95.	.0020	80.
pixel only	156.		156.

Table 1: Resolution in reconstructed Cerenkov angle θ_C (RICH 1). The resolutions obtained fitting the data points on the particle *orthogonal plane* are shown in rows 1, with, and 2, without corrections Δb; in row 3 there is the result of the direct fit on the detector plane; row 4 shows for comparison the resolution obtained with the method of the direct emission angle reconstruction; in row 5 the order of magnitude of the contribution due to the experimental resolution (to be added in quadrature). See the text for details.

b) For comparison, a more crude approach is to fit directly a circle to the data points on the detector plane. In this case the goodness of the fit is much worse than in the case of the ellipse. The fitted radius (r_f) is then corrected for the angle the $reflected\ particle$ makes with the detector plane (i.e. it is projected on the *orthogonal plane*); then θ_C is computed dividing r_f by d_{md}; the resolution is quite poor, but an empirical correction as a function of the particle *impact parameter* can be further applied with a nice increase in the resolution; the result is shown in the third row of table 1.